



Analysis of Zero-Hopf Bifurcation in Two Rössler Systems Using Normal Form Theory

Bing Zeng^{*,†,‡} and Pei Yu^{†,§}

^{*}*School of Mathematics and Statistics, Lingnan Normal University,
Zhanjiang, Guangdong 524048, P. R. China*

[†]*Department of Applied Mathematics, Western University,
London, Ontario, N6A 5B7, Canada*

[‡]*zengb@lingnan.edu.cn*

[§]*pyu@uwo.ca*

Received May 27, 2020

In recent publications [Llibre, 2014; Llibre & Makhlof, 2020], time-averaging method was applied to studying periodic orbits bifurcating from zero-Hopf critical points of two Rössler systems. It was shown that the averaging method is successful for a certain type of zero-Hopf critical points, but fails for some type of such critical points. In this paper, we apply normal form theory to reinvestigate the bifurcation and show that the method of normal forms is applicable for all types of zero-Hopf bifurcations, revealing why the time-averaging method fails for some type of zero-Hopf bifurcation.

Keywords: Rössler system; zero-Hopf bifurcation; normal form; periodic orbit; limit cycle.

1. Introduction

Recently, Llibre and Makhlof [2020] applied the time-averaging method to analyze zero-Hopf bifurcation in a Rössler system and obtained periodic orbits around such a critical point. However, they also showed that the time-averaging method cannot be used to detect periodic orbits around a certain type of such critical points. The Rössler system considered in [Llibre & Makhlof, 2020] is given by

$$\begin{aligned} \dot{x} &= x - xy - z, \\ \dot{y} &= x^2 - a_1y, \\ \dot{z} &= b_1(c_1x - z), \end{aligned} \quad (1)$$

where the dot denotes differentiation with respect to time, a_1 , b_1 , and c_1 are real parameters. Earlier, Llibre [2014] also studied zero-Hopf bifurcation in another Rössler system, described by

$$\dot{x} = -y - z,$$

$$\begin{aligned} \dot{y} &= x + a_2y, \\ \dot{z} &= b_2x - c_2z + xz, \end{aligned} \quad (2)$$

where a_2 , b_2 , and c_2 are also real parameters. The most well-known Rössler system proposed by Rössler [1976] is given as follows (also see [Yu & Chen, 2004] for chaos control of this system):

$$\begin{aligned} \dot{x} &= -y - z, \\ \dot{y} &= x + a_3y, \\ \dot{z} &= b_3 + z(x - c_3), \end{aligned} \quad (3)$$

where a_3 , b_3 , and c_3 are real parameters. All the three different Rössler systems have multiple equilibria, and both Hopf and zero-Hopf bifurcations can occur from these equilibria. It is noted that systems (2) and (3) have two equilibria, while system (1) has three equilibria. We can show that system (3) is actually equivalent to system (2) or

[§]Author for correspondence

more precisely system (2) is more general than system (3). To prove this, first, it is easy to find the two equilibria of system (3), given by

$$E_{\pm} = (x_e, y_e, z_e),$$

where

$$y_e = \frac{-c_3 \pm \sqrt{c_3^2 - 4a_3b_3}}{2a_3}, \quad x_e = -a_3y_e,$$

$$z_e = -y_e, \quad (a_3 \neq 0, c_3^2 \geq 4a_3b_3).$$

When $c_3^2 = 4a_3b_3$, the two equilibria E_{\pm} have coincided into one with $y_e = -\frac{2b_3}{c_3}$, $c_3 \neq 0$. Then, shifting E_{\pm} to the origin and letting

$$a_3 = a_2, \quad \frac{c_3 \pm \sqrt{c_3^2 - 4a_3b_3}}{2a_3} = b_2, \quad a_3b_2 = c_2,$$

we obtain system (2). The equivalence of systems (2) and (3) is also mentioned in [Llibre, 2014]. But the systems (1) and (2) are not equivalent since there does not exist a linear or nonlinear transformation between these two systems, by noticing that these two systems have a different number of equilibria. Therefore, in the following analysis, our study is focused on systems (1) and (2).

In [Llibre & Makhlof, 2020] the authors have shown that system (1) can have zero-Hopf bifurcation at the three equilibria and they applied time-averaging to detect possible periodic orbits. In particular, they used the time-averaging method to obtain the periodic solutions around the equilibrium at the origin, but could not detect possible periodic solutions around the other two nonzero equilibria. Similarly, Llibre [2014] considered system (2), which has two equilibria and the dynamical property around them is the same, and showed that zero-Hopf bifurcation occurs for a certain set of parameter values. However, Llibre again found that the time-averaging method can be used to detect periodic orbits for a subset of the parameter values, but could not for the remaining subset of the parameter values.

In this paper, we will apply normal form theory to reinvestigate the zero-Hopf bifurcations in the two Rössler systems (1) and (2). It is well known that center manifold theory and normal form theory are very powerful mathematical tools in analyzing local bifurcations of dynamical systems such as saddle-node bifurcation, Hopf bifurcation, zero-Hopf bifurcation, and Bogdanov–Takens bifurcation, etc., see [Guckenheimer & Holmes, 1993;

Kuznetsov, 2004; Han & Yu, 2012]. In the past few decades, efficient methods for computing center manifold and normal forms using computer algebra systems such as Maple and Mathematica have been developed, for example, see [Yu, 1998; Bi & Yu, 1999; Han & Yu, 2012; Tian & Yu, 2014]. Especially, the symbolic programs using Maple for semi-simple cases can be found in [Bi & Yu, 1999; Tian & Yu, 2014], which contain zero-Hopf bifurcation. In these symbolic programs, center manifold theory and normal form theory are combined in a utilized algorithm to yield one-step nonlinear transformation and normal form simultaneously. Suppose for a general dynamical system,

$$\dot{\mathbf{x}} = J(\boldsymbol{\mu})\mathbf{x} + \mathbf{f}(\mathbf{x}, \boldsymbol{\mu}), \quad \mathbf{x} \in \mathbb{R}^n, \quad \boldsymbol{\mu} \in \mathbb{R}^k, \quad (4)$$

where \mathbf{x} and $\boldsymbol{\mu}$ are n -d state vector and k -d parameter vector respectively, $J(\boldsymbol{\mu})\mathbf{x}$ and $\mathbf{f}(\mathbf{x}, \boldsymbol{\mu})$ represent the linear and nonlinear parts of the system, satisfying $\mathbf{f}(\mathbf{0}, \boldsymbol{\mu}) = \mathbf{0}$. Further, assume that at the critical point $\boldsymbol{\mu} = \mathbf{0}$, the Jacobian $J(\mathbf{0})$ of the system contains a single zero and a purely imaginary pair, put in the Jordan canonical form,

$$J(\mathbf{0}) = \begin{bmatrix} 0 & 0 & 0 & 0 \\ 0 & 0 & \omega_c & 0 \\ 0 & -\omega_c & 0 & 0 \\ 0 & 0 & 0 & A \end{bmatrix},$$

where $\omega_c > 0$ and A is an $(n - 3) \times (n - 3)$ stable matrix (i.e. all eigenvalues of A have the negative real part). Then applying the Maple program [Bi & Yu, 1999; Tian & Yu, 2014] to system (4) we obtain the following normal form expressed in cylindrical coordinates [Yu & Yuan, 2001]:

$$\begin{aligned} \dot{w} &= a_{100}\beta_1 + a_{120}w^2 + a_{102}r^2 + a_{130}w^3 \\ &\quad + a_{112}wr^2 + \dots, \\ \dot{r} &= a_{200}\beta_2 + a_{211}wr + a_{221}w^2r + a_{203}r^3 + \dots, \\ \dot{\theta} &= \omega_c + a_{300}\beta_3 + a_{310}w + a_{320}w^2 + a_{302}r^2 + \dots, \end{aligned} \quad (5)$$

where the coefficients a_{ijk} are explicitly expressed in terms of the original parameters evaluated at $\boldsymbol{\mu} = \mathbf{0}$, and β_j , $j = 1, 2, 3$ are given in terms of $\boldsymbol{\mu}$. For generic zero-Hopf bifurcation, the codimension of the unfolding is two.

In this paper, the normal form computation method with the normal form associated with zero-Hopf bifurcation will be used to study the zero-Hopf

bifurcations in the Rössler systems (1) and (2). It will be shown that the periodic orbits bifurcating from the zero-Hopf critical points, detected by the time-averaging method [Llibre & Makhlouf, 2020] are stable periodic orbits, while those that cannot be detected in [Llibre, 2014; Llibre & Makhlouf, 2020] are unstable solutions or the critical zero-Hopf bifurcation point may be a center or undeterminable. In the next section, the Rössler system (1) is analyzed, and the Rössler system (2) is considered in Sec. 3. The conclusion is given in Sec. 4.

2. Zero-Hopf Bifurcation in the Rössler System (1)

In this section, we consider zero-Hopf bifurcation in the Rössler system (1). First, the three equilibria of (1) can be easily obtained as

$$\begin{aligned} E_0 &= (0, 0, 0), \\ E_{\pm} &= (\pm\sqrt{a_1(1-c_1)}, 1-c_1, \\ &\quad \pm c_1\sqrt{a_1(1-c_1)}), \quad \text{for } a_1(1-c_1) > 0. \end{aligned} \tag{6}$$

Next, note that when $a_1(1-c) > 0$, applying the following shifting,

$$\begin{aligned} x &\rightarrow \pm(\sqrt{a_1(1-c_1)} + x), \\ y &\rightarrow (1-c_1) + y, \\ z &\rightarrow \pm(c_1\sqrt{a_1(1-c_1)} + z), \end{aligned}$$

to E_{\pm} yields an exactly same system. Therefore, we shall only consider zero-Hopf bifurcation from E_0 and E_+ , knowing that the local dynamics around E_+ must exactly occur around E_- . In particular, the (stable or unstable) periodic orbits to be obtained around E_+ must also appear around E_- .

2.1. Zero-Hopf bifurcation at E_0

We first consider the equilibrium E_0 . Evaluating the Jacobian of (1) at E_0 gives the characteristic polynomial,

$$P_0(\lambda) = (\lambda + a_1)[\lambda^2 + (b_1 - 1)\lambda + b_1(c_1 - 1)],$$

which implies that a zero-Hopf bifurcation occurs at $a_1 = 0$ and $b_1 = 1$ with $c_1 > 1$. We have the following theorem.

Theorem 1. *The equilibrium E_0 of system (1) is asymptotically stable for $a_1 > 0$, $b_1 > 1$ and $c_1 > 1$,*

and zero-Hopf bifurcation occurs from E_0 at the critical point $a_1 = 0$, $b_1 = 1$ ($c_1 > 1$). In the vicinity of this critical point, supercritical Hopf bifurcation can occur when $b_1 = 1$, yielding stable bifurcating limit cycles.

Proof. Define the zero-Hopf critical point as

$$C_0 : a_{1c} = 0, \quad b_{1c} = 1 \quad (c_1 > 1), \tag{7}$$

for which the eigenvalues associated with the critical point C_0 are $0, \pm i\omega_c$, where $\omega_c = \sqrt{c_1 - 1}$. Further, perturbing the critical point C_0 , we may let

$$\begin{aligned} a_1 &= a_{1c} + \mu_1 = \mu_1, \\ b_1 &= b_{1c} + \mu_2 = 1 + \mu_2, \\ 0 &< \mu_1, \quad |\mu_2| \ll 1. \end{aligned} \tag{8}$$

Then, introducing the linear transformation,

$$\begin{pmatrix} x \\ y \\ z \end{pmatrix} = \begin{bmatrix} \frac{1}{c_1} & \frac{\sqrt{c_1-1}}{c_1} & 0 \\ 0 & 0 & 1 \\ 1 & 0 & 0 \end{bmatrix} \begin{pmatrix} u \\ v \\ w \end{pmatrix}$$

into (1) we obtain

$$\begin{aligned} \dot{w} &= -\mu_1 w + \frac{1}{c_1^2} u^2 + \frac{c_1 - 1}{c_1^2} v^2 + \frac{2\sqrt{c_1 - 1}}{c_1^2} uv, \\ \dot{u} &= \sqrt{c_1 - 1} \mu_2 v + \sqrt{c_1 - 1} v, \\ \dot{v} &= -\mu_2 v - \sqrt{c_1 - 1} u - \frac{1}{\sqrt{c_1 - 1}} w u - w v, \end{aligned} \tag{9}$$

where the perturbation parameters μ_1 and μ_2 are also called unfolding. Note that higher-order terms involving μ_1 and μ_2 are ignored.

Now, setting $\mu_1 = \mu_2 = 0$ and applying the Maple program in [Bi & Yu, 1999] or [Tian & Yu, 2014] to system (9) we obtain the following normal form with the unfolding added (for convenience, the notation w is still used in the normal form),

$$\begin{aligned} \dot{w} &= -\mu_1 w + \frac{1}{2c_1} r^2 - \frac{1}{4c_1(c_1 - 1)} w r^2, \\ \dot{r} &= -\frac{1}{2} \mu_2 r - \frac{1}{2} w r + \frac{1}{16c_1(c_1 - 1)} r^3, \\ \dot{\theta} &= \sqrt{c_1 - 1} + \frac{1}{2} \sqrt{c_1 - 1} \mu_2 + \frac{1}{2\sqrt{c_1 - 1}} w \\ &\quad - \frac{c_1}{8\sqrt[3]{(c_1 - 1)^2}} w^2 + \frac{1}{16c_1\sqrt{c_1 - 1}} r^2. \end{aligned} \tag{10}$$

The first two equations in the normal form (10) can be used for bifurcation analysis, while the third equation can be used to determine the frequency of periodic solutions.

Letting $\dot{w} = \dot{r} = 0$ in (10) yields two *steady-state* solutions, one of them is $(w, r) = (0, 0)$, which is actually the equilibrium solution E_0 of system (1). The other steady-state solution is given by $(w, r) = (w_s, r_s)$, where

$$w_s = -\mu_2 + \frac{r_s^2}{8c_1(c_1 - 1)}, \quad (11)$$

and r_s^2 is determined from the quadratic polynomial in r_s^2 ,

$$r_s^4 - 4c_1(c_1 - 1)[4(c_1 - 1) + 2\mu_2 - \mu_1]r_s^2 - 32c_1^2(c_1 - 1)^2\mu_1\mu_2 = 0,$$

which gives possible solutions for r_s^2 :

$$r_{s\pm}^2 = 2c_1(c_1 - 1)[4(c_1 - 1) + 2\mu_2 - \mu_1] \pm \sqrt{[4(c_1 - 1) + 2\mu_2 - \mu_1]^2 + 8\mu_1\mu_2}. \quad (12)$$

It follows from $\mu_1 > 0$ that when $\mu_2 > 0$, there exists only one positive solution r_{s+}^2 . When $\mu_2 < 0$, there exist either no positive solution or two positive solutions $r_{s\pm}$ if

$$4(c_1 - 1) + 2\mu_2 - \mu_1 > 0 \quad \text{and} \\ [4(c_1 - 1) + 2\mu_2 - \mu_1]^2 + 8\mu_1\mu_2 > 0,$$

which needs

$$4(c_1 - 1) + 2\mu_2 - \mu_1 > 2\sqrt{-2\mu_1\mu_2} \\ \Rightarrow \sqrt{\mu_1} + \sqrt{-2\mu_2} < 2\sqrt{c_1 - 1}. \quad (13)$$

Note that a possible solution of $r_{s\pm}^2$, for which the corresponding component w_s is given by (11), represents a periodic orbit in the original three-dimensional x - y - z space. In general, this type of periodic orbits is different from that bifurcating from a Hopf critical point, associated with a pair of purely imaginary eigenvalues. However, in the vicinity of a generic zero-Hopf bifurcation point, there exist Hopf bifurcation and one-dimensional bifurcations such as saddle-node bifurcation, and so such periodic orbits may be limit cycles if they indeed bifurcate from a Hopf bifurcation curve. It will be seen that this is true for the Rössler system (1). Therefore, the periodic orbits detected in [Llibre & Makhlof, 2020] are limit cycles.

The stability of the two steady-state solutions are determined by the Jacobian of the first two equations of (10), evaluated at $(w, r) = (0, 0)$ resulting in two eigenvalues: $-\mu_1 < 0$ and $-\frac{\mu_2}{2}$. So the solution $(w, r) = (0, 0)$ [i.e. the equilibrium E_0 of (1)] is stable (unstable) if $\mu_2 > 0$ (< 0). To find the stability of the periodic orbits (w_{s+}, r_{s+}) , evaluating the Jacobian at (w_{s+}, r_{s+}) yields the determinant, given by

$$\det_+ = -\frac{1}{4}\{[4(c_1 - 1) + 2\mu_2 - \mu_1]^2 + 8\mu_1\mu_2 + [4(c_1 - 1) + 2\mu_2 - \mu_1] \times \sqrt{[4(c_1 - 1) + 2\mu_2 - \mu_1]^2 + 8\mu_1\mu_2}\},$$

which implies that $\det_+ < 0$ for the periodic solution (r_{s+}, w_{s+}) no matter whether $\mu_2 > 0$ or $\mu_2 < 0$. Thus, the periodic solution (w_{s+}, r_{s+}) is unstable as long as it exists.

To find the stability of (w_{s-}, r_{s-}) , similarly, we obtain

$$\det_- = -\frac{1}{4}\{[4(c_1 - 1) + 2\mu_2 - \mu_1]^2 + 8\mu_1\mu_2 - [4(c_1 - 1) + 2\mu_2 - \mu_1] \times \sqrt{[4(c_1 - 1) + 2\mu_2 - \mu_1]^2 + 8\mu_1\mu_2}\} \\ = \frac{1}{4}\sqrt{[4(c_1 - 1) + 2\mu_2 - \mu_1]^2 + 8\mu_1\mu_2} \times \{4(c_1 - 1) + 2\mu_2 - \mu_1 - \sqrt{[4(c_1 - 1) + 2\mu_2 - \mu_1]^2 + 8\mu_1\mu_2}\} \\ > 0 \quad \text{for } \mu_1 > 0 \text{ and } \mu_2 < 0.$$

Hence, the stability of the periodic orbit (w_{s-}, r_{s-}) is determined by the trace, given below:

$$\text{Tr}_- = -\mu_1 - \frac{1}{4}\{4(c_1 - 1) + 2\mu_2 - \mu_1 - \sqrt{[4(c_1 - 1) + 2\mu_2 - \mu_1]^2 + 8\mu_1\mu_2}\} < 0,$$

indicating that the periodic orbit (w_{s-}, r_{s-}) is stable when $\mu_1 > 0$, $\mu_2 < 0$, and the condition (13) holds. ■

It is seen from the bifurcation diagram as shown in Fig. 1 that E_0 is stable for (μ_1, μ_2) taking values from the first quadrant in the μ_1 - μ_2 parameter plane. Hopf bifurcation occurs from the μ_1 -axis

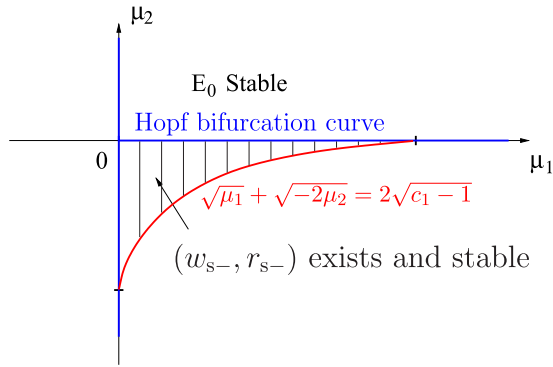


Fig. 1. Zero-Hopf bifurcation diagrams of system (1) at E_0 .

($\mu_2 = 0, \mu_1 > 0$), which is indicated as “Hopf bifurcation curve” in this figure, and the bifurcating limit cycles are stable for the parameter values from the shaded region, bounded by the μ_1 -axis, the μ_2 -axis, and the curve $\sqrt{\mu_1} + \sqrt{-2\mu_2} = 2\sqrt{c_1 - 1}$ based on the condition (13) (the red curve in the figure). It is obvious that the condition (13) is always satisfied if $c_1 - 1 = O(1)$. When $\mu_1 = O(\varepsilon)$, $\mu_2 = O(\varepsilon)$ and $c_1 - 1 = O(\varepsilon)$, the condition (13) is required for the existence and stability of the limit cycle solution (w_{s-}, r_{s-}).

A numerical example was given in [Llibre & Makhlof, 2020] to show a stable limit cycle around the origin. Using our notation, the parameter values taken in [Llibre & Makhlof, 2020] are

$$c_1 = 2, \quad \mu_1 = 0.01, \quad \mu_2 = -0.005, \quad \text{and so}$$

$$a_1 = 0.01, \quad b_1 = 1 - 0.005 = 0.995.$$

It is easy to see that the condition (13) is satisfied with the above parameter values since $c_1 = 2$. Using

the above formulas, we obtain

$$w_{s-} = 0.00501256, \quad r_{s-} = 0.01417729,$$

$$\omega = 1.00000628,$$

where ω is the frequency of the bifurcating limit cycle. To verify the stability of the limit cycle, we calculate the eigenvalues of the Jacobian of the first two equations of (10) and evaluate it at the above solution to obtain $-0.00500628 \pm 0.00499372i$, which indeed indicates that the bifurcating limit cycle is stable.

To end this subsection, we present a numerical example for a small value of $c_1 - 1$, with the values of μ_1 and μ_2 taken close to the boundary $\sqrt{\mu_1} + \sqrt{-2\mu_2} = 2\sqrt{c_1 - 1}$. The parameter values we choose are

$$c_1 = 1.0625, \quad \mu_1 = 0.05, \quad \mu_2 = -0.035, \quad \text{and so}$$

$$a_1 = 0.05, \quad b_1 = 1 - 0.035 = 0.965.$$

Again, applying the above formulas yields

$$w_{s-} = 0.05403709, \quad r_{s-} = 0.10056567,$$

$$\omega = 0.318133754.$$

The simulation is shown in Fig. 2, with initial conditions $(x, y, z) = (0.019, 0.021, 0.012)$ and $(0.5, 0.5, 0.5)$ chosen for Figs. 2(a) and 2(b), respectively. Both the simulated trajectories converge to the same stable limit cycle. Even if the initial point is chosen as $(x, y, z) = (1, 1, 1)$, the trajectory still converges to the stable limit cycle. This seems to suggest that the limit cycle is globally asymptotically stable, though it cannot be proved theoretically.

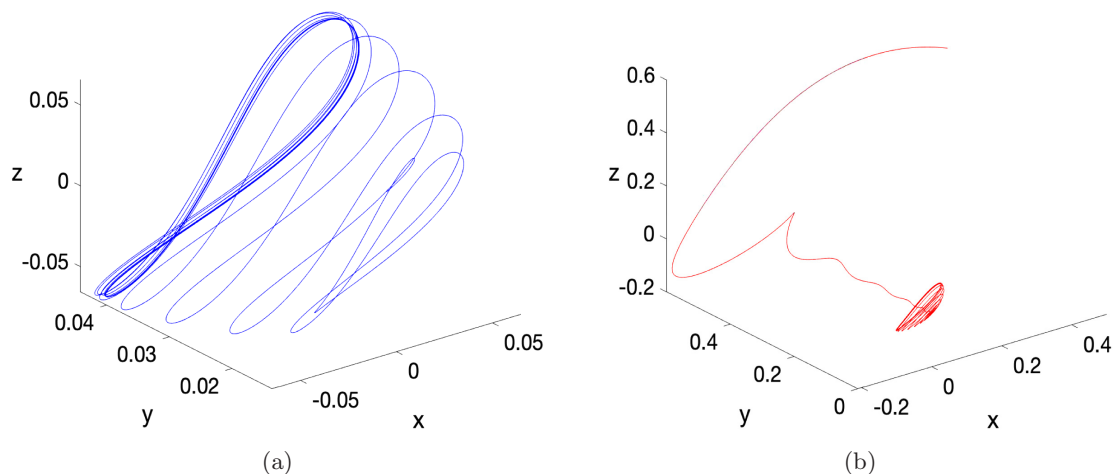


Fig. 2. Simulations of system (1) for $a_1 = 0.05$, $b_1 = 0.965$, $c_1 = 1.0625$, converging to the stable limit cycle with the initial conditions: (a) $(x_0, y_0, z_0) = (0.019, 0.021, 0.012)$ and (b) $(x_0, y_0, z_0) = (0.5, 0.5, 0.5)$.

It is seen from Fig. 2(a) that the simulation agrees very well with the theoretical prediction.

2.2. Zero-Hopf bifurcation at E_+

We now turn to consider the equilibrium E_+ which exists under the condition $a_1(1 - c_1) > 0$. We have the following result.

Theorem 2. *The equilibrium E_+ of system (1) is asymptotically stable for*

$$\begin{aligned} a_1 + b_1 - c_1 &> 0, \\ b_1 &> 0, \\ (a_1 + b_1 - c_1)a_1(b_1 - 3c_1 + 2) \\ &- 2a_1b_1(1 - c_1) > 0, \end{aligned} \tag{14}$$

and zero-Hopf bifurcation occurs from E_+ at the critical point $b_1 = 0, c_1 = a_1 (a_1(2 - 3a_1) > 0)$. In the vicinity of this critical point, subcritical Hopf bifurcation occurs, yielding unstable bifurcating limit cycles.

Proof. Evaluating the Jacobian of system (1) at E_+ gives

$$\begin{aligned} P_+(\lambda) &= \lambda^3 + (a_1 + b_1 - c_1)\lambda^2 \\ &\quad + a_1(b_1 - 3c_1 + 2)\lambda + 2a_1b_1(1 - c_1). \end{aligned}$$

Thus, the equilibrium E_+ , which exists for $a_1(1 - c_1) > 0$, is stable when the conditions given in (14) hold. Zero-Hopf bifurcation occurs at the critical point C_1 , defined as

$$\begin{aligned} C_1 : \quad b_{1c} &= 0, \quad c_{1c} = a_1, \quad \text{with} \\ a_1(2 - 3a_1) &> 0 \text{ or } 0 < a_1 < \frac{2}{3}. \end{aligned} \tag{15}$$

Perturbing the critical point C_1 , we let

$$\begin{aligned} b_1 &= b_{1c} + \mu_1 = \mu_1, \\ c_1 &= c_{1c} + \mu_2 = a_1 + \mu_2, \\ 0 < a_1 < \frac{2}{3}, \quad 0 < \mu_1, \quad |\mu_2| &\ll 1. \end{aligned} \tag{16}$$

Next, applying the following affine transformation,

$$\begin{pmatrix} x \\ y \\ z \end{pmatrix} = \begin{pmatrix} \sqrt{a_1(1 - c_1)} \\ 1 - c_1 \\ c_1 \sqrt{a_1(1 - c_1)} \end{pmatrix} + \begin{bmatrix} \frac{\sqrt{a_1(1 - a_1)}}{2(1 - a_1)} & \frac{\sqrt{a_1(1 - a_1)}(2 - 3a_1)}{2a_1(1 - a_1)} & \frac{1}{3a_1 - 2} \\ 1 & 0 & \frac{2\sqrt{a_1(1 - a_1)}}{a_1(3a_1 - 2)} \\ 0 & 0 & 1 \end{bmatrix} \begin{pmatrix} u \\ v \\ w \end{pmatrix}$$

into system (1) yields

$$\begin{aligned} \dot{w} &= -\frac{2(1 - a_1)}{2 - 3a_1}\mu_1 w, \\ \dot{u} &= \sqrt{a_1(2 - 3a_1)}u + \left(\frac{a_1}{2 - 3a_1}\mu_1 - \frac{a_1}{2(1 - a_1)}\mu_2\right)u + \left(\frac{\sqrt{a_1}}{\sqrt{2 - 3a_1}}\mu_1 - \frac{\sqrt{a_1(2 - 3a_1)}}{2(1 - a_1)}\mu_2\right)v + \frac{a_1}{4(1 - a_1)}u^2 \\ &\quad + \frac{2 - 3a_1}{4(1 - a_1)}v^2 + \frac{1}{(2 - 3a_1)^2}w^2 + \frac{\sqrt{a_1(2 - 3a_1)}}{2(1 - a_1)}uw - \frac{\sqrt{a_1(1 - a_1)}}{(1 - a_1)(2 - 3a_1)}wu - \frac{1}{(1 - a_1)(2 - 3a_1)}wv, \\ \dot{v} &= -\sqrt{a_1(2 - 3a_1)}u + \frac{(4 - 3a_1)\sqrt{a_1}}{2(1 - a_1)\sqrt{2 - 3a_1}}\mu_2 u + \frac{2 - a_1}{2(1 - a_1)}\mu_2 v - \frac{(4 - 3a_1)\sqrt{a_1}}{4(1 - a_1)\sqrt{2 - 3a_1}}u^2 - \frac{\sqrt{a_1(2 - 3a_1)}}{4(1 - a_1)}v^2 \\ &\quad - \frac{(4 - 3a_1)\sqrt{a_1(2 - 3a_1)}}{a_1(2 - 3a_1)^3}w^2 - \frac{2 - a_1}{2(1 - a_1)}uw + \frac{(4 - 3a_1)\sqrt{a_1(2 - 3a_1)}}{(2 - 3a_1)^2\sqrt{a_1(1 - a_1)}}wu + \frac{2 - a_1}{(2 - 3a_1)\sqrt{a_1(1 - a_1)}}wv, \end{aligned} \tag{17}$$

where μ_1 and μ_2 are perturbation parameters (unfolding), and higher-order terms containing μ_1 and μ_2 are dropped. It is easy to see from the first equation of (17), which does not contain any terms except the

linear perturbation term, that the normal form of this system is equivalent to that of Hopf bifurcation. Applying the Maple program [Yu, 1998] to system (17) we obtain the following normal form [including the first equation of (17)]:

$$\begin{aligned} \dot{w} &= -\frac{2(1-a_1)}{2-3a_1}\mu_1 w, \\ \dot{r} &= \frac{1}{2}\left(\frac{a_1}{2-3a_1}\mu_1 + \mu_2\right)r + \frac{3}{16(2-3a_1)}r^3, \\ \dot{\theta} &= \sqrt{a_1(2-3a_1)} + \frac{1}{2}\sqrt{\frac{a_1}{2-3a_1}}\mu_1 \\ &\quad - \frac{3}{2}\sqrt{\frac{a_1}{2-3a_1}}\mu_2 - \frac{21a_1+16}{48(2-3a_1)\sqrt{2-3a_1}}r^2. \end{aligned} \tag{18}$$

The w equation is decoupled from r and θ equations. Because $\mu_1 > 0$, and $0 < a_1 < \frac{2}{3}$, $w = 0$ is stable. Further, it is seen from the second equation of (18) that the coefficient of r^3 is positive, implying that the Hopf bifurcation is subcritical and so the bifurcating limit cycles are unstable. That is why the averaging method cannot be used to detect periodic orbits around the equilibrium E_1 [Llibre & Makhlof, 2020], since the time-averaging method cannot detect unstable limit cycles. ■

3. Zero-Hopf Bifurcation in the Rössler System (2)

In this section, we study the second Rössler system (2), which has been studied by Llibre [2014] and formulas for periodic orbits were derived, which again showed that the time-averaging method cannot detect unstable limit cycles. System (2) has two equilibria:

$$E_0 = (0, 0, 0) \quad \text{and}$$

$$E_1 = \left(c_2 - a_2 b_2, b_2 - \frac{c_2}{a_2}, \frac{c_2}{a_2} - b_2\right), \quad (a_2 \neq 0). \tag{19}$$

A direct computation shows that shifting the system from E_1 to the origin and letting $a = \bar{a}$, $\frac{c}{a} = \bar{b}$, $ab = \bar{c}$ yield the system (2). Therefore, we only need to consider the equilibrium E_0 . Evaluating the Jacobian of (2) at E_0 leads to the characteristic polynomial,

$$\begin{aligned} P_0(\lambda) &= \lambda^3 + (c_2 - a_2)\lambda^2 + (1 + b_2 - a_2 c_2)\lambda \\ &\quad + c_2 - a_2 b_2. \end{aligned}$$

Zero-Hopf bifurcation occurs if $c_2 - a_2 = 0$, $c_2 - a_2 b_2 = 0$ and $1 + b_2 - a_2 c_2 > 0$. There are two cases:

Case (A). $-\sqrt{2} < a_2 = c_2 \neq 0 < \sqrt{2}$, $b_2 = 1$;

Case (B). $a_2 = c_2 = 0$, $b_2 > -1$.

(20)

We first consider Case (A) and then Case (B).

It should be noted that the conditions for system (2) to have zero-Hopf bifurcation at the equilibrium E_1 are exactly the same as those given in Case (A). Thus, the analysis given in the following subsections can also be applied to study the equilibrium E_1 .

3.1. Zero-Hopf bifurcation at E_0 for Case (A)

Regarding the zero-Hopf bifurcation of system (2) for Case (A), we have the following theorem.

Theorem 3. *The equilibrium E_0 of system (2) is asymptotically stable for $c_2 > \max\{a_2, a_2 b_2\}$, $1 + b_2 - a_2 c_2 > 0$. Zero-Hopf bifurcation occurs from E_0 at the critical point $b_2 = 1$, $c_2 = a_2$ ($a_2^2 < 2$). Static bifurcation occurs in the vicinity of this critical point, yielding nonzero equilibrium solution E_1 . Hopf bifurcation is not possible and no periodic solutions are found around this zero-Hopf critical point.*

Proof. Define the perturbation as

$$\begin{aligned} C_0 : \quad b_2 &= 1 + \mu_1, \quad c_2 = a_2 + \mu_2, \\ a_2^2 &< 2, \quad 0 < |\mu_1|, \quad |\mu_2| \ll 1. \end{aligned} \tag{21}$$

Introducing the linear transformation,

$$\begin{pmatrix} x \\ y \\ z \end{pmatrix} = \begin{bmatrix} a_2 & \sqrt{2-a_2^2} & a_2 \\ 1-a_2^2 & -a_2\sqrt{2-a_2^2} & -1 \\ 1 & 0 & 1 \end{bmatrix} \begin{pmatrix} u \\ v \\ w \end{pmatrix} \tag{22}$$

into system (2) we have

$$\begin{aligned} \dot{w} &= \left(\frac{a_2}{2-a_2^2}\mu_1 - \frac{1}{2-a_2^2}\mu_2\right)w \\ &\quad + \frac{a_2}{2-a_2^2}(u+w)^2 + \frac{1}{\sqrt{2-a_2^2}}(u+w)v, \end{aligned}$$

$$\begin{aligned}
 \dot{u} &= \sqrt{2 - a_2^2}v + \frac{1 - a_2^2}{2 - a_2^2}(a_2\mu_1 - \mu_2)u \\
 &\quad + \frac{1 - a_2^2}{\sqrt{2 - a_2^2}}\mu_1v + \frac{a_2(1 - a_2^2)}{2 - a_2^2}(u + w)^2 \\
 &\quad + \frac{1 - a_2^2}{\sqrt{2 - a_2^2}}(u + w)v, \\
 \dot{v} &= -\sqrt{2 - a_2^2}u - \frac{a_2}{\sqrt{2 - a_2^2}}(a_2\mu_1 + \mu_2)u \\
 &\quad - a_2\mu_1v - \frac{a_2^2}{\sqrt{2 - a_2^2}}(u + w)^2 \\
 &\quad - a_2(u + w)v.
 \end{aligned} \tag{23}$$

Now applying the Maple program [Bi & Yu, 1999; Tian & Yu, 2014] to system (23) we obtain the following normal form,

$$\begin{aligned}
 \dot{w} &= \frac{1}{2 - a_2^2} \left[(a_2\mu_1 - \mu_2)w + a_2w^2 + \frac{a_2}{2}r^2 \right], \\
 \dot{r} &= -\frac{1}{2(2 - a_2^2)}r \left[a_2\mu_1 + (1 - a_2^2)\mu_2 \right. \\
 &\quad \left. + a_2^3w - \frac{1 + 4a_2^2}{8a_2^2(2 - a_2^2)}r^2 \right], \\
 \dot{\theta} &= \sqrt{2 - a_2^2} + \frac{1}{2\sqrt{2 - a_2^2}}(\mu_1 - a_2\mu_2) \\
 &\quad + \frac{1 + a_2^2}{2\sqrt{2 - a_2^2}}w + \frac{1}{48(2 - a_2^2)^{5/2}}[24(1 + a_2^2)
 \end{aligned}$$

$$\begin{aligned}
 &\times (2 - a_2^2)^2w - 6(2 + 19a_2^2 - 16a_2^4)w^2 \\
 &\quad - (10 + 21a_2^2 - 12a_2^4)r^2].
 \end{aligned} \tag{24}$$

The first two equations of (24) are used for bifurcation analysis. Setting $\dot{w} = \dot{r} = 0$ yields three steady-state solutions:

$$\begin{aligned}
 S_0 &: (w_0, r_0) = (0, 0), \\
 S_1 &: (w_1, r_1) = \left(-\mu_1 + \frac{1}{a_2}\mu_2, 0 \right), \\
 S_2 &: (w_2, r_2),
 \end{aligned} \tag{25}$$

where

$$w_2 = \frac{1}{a_2^3} \left(-a_2\mu_1 - (1 - a_2^2)\mu_2 + \frac{a_2(1 + 4a_2^2)}{8(2 - a_2^2)}r^2 \right), \tag{26}$$

and r_2^2 is determined from the following quadratic polynomial equation,

$$\begin{aligned}
 r_2^4 + A_1r_2^2 + A_2 &= 0, \quad \text{where} \\
 A_1 &= \frac{32a_2^4(2 - a_2^2)^2}{(1 + 4a_2^2)^2} - \frac{8(2 - a_2^2)^2}{a_2(1 + 4a_2^2)}(a_2\mu_1 + \mu_2), \\
 A_2 &= \frac{64(2 - a_2^2)^2}{a_2^2(1 + 4a_2^2)^2} [a_2\mu_1 + (1 - a_2^2)\mu_2] \\
 &\quad \times [a_2(1 - a_2^2)\mu_1 + \mu_2].
 \end{aligned} \tag{27}$$

It is obvious to see that $S_0 = E_0$. Further, it is easy to use (21) and (22) to prove that $S_1 = E_1$.

Let the Jacobian of the first two equations of (24) be $J(w, r)$. Then, $J(S_0)$ gives

$$J(S_0) = J(0, 0) = \begin{bmatrix} \frac{1}{2 - a_2^2}(a_2\mu_1 - \mu_2) & 0 \\ 0 & -\frac{1}{2(2 - a_2^2)}(a_2\mu_1 + (1 - a_2^2)\mu_2) \end{bmatrix}.$$

Thus, S_0 (i.e. the E_0) is asymptotically stable if

$$a_2\mu_1 - \mu_2 < 0 \quad \text{and} \quad a_2\mu_1 + (1 - a_2^2)\mu_2 > 0 \Rightarrow -(1 - a_2^2)\mu_2 < a\mu_1 < \mu_2,$$

which implies $\mu_2 > 0$ since $a_2^2 < 2$. The above two inequalities define two critical bifurcation lines in the μ_1 - μ_2 plane:

$$L_1 : a_2\mu_1 - \mu_2 = 0 \quad \text{and} \quad L_2 : a_2\mu_1 + (1 - a_2^2)\mu_2 = 0. \tag{28}$$

Similarly, evaluating $J(S_1)$ we obtain

$$J(S_1) = J(w_1, 0) = \begin{bmatrix} -\frac{1}{2-a_2^2}(a_2\mu_1 - \mu_2) & 0 \\ 0 & -\frac{1}{2(2-a_2^2)}(a_2\mu_1 + (1-a_2^2)\mu_2) \end{bmatrix},$$

which indicates that S_1 (i.e. the E_2) is asymptotically stable if

$$a_2\mu_1 - \mu_2 > 0 \quad \text{and} \quad a_2\mu_1 + (1-a_2^2)\mu_2 > 0.$$

Comparing the stability of E_1 with that of E_0 we see that there exists a *static bifurcation* between E_0 and E_1 from the critical line L_1 . Moreover, Hopf bifurcations may possibly occur from the equilibrium solution E_0 or E_1 on the critical line L_2 . The Hopf bifurcation from E_0 is so-called *incipient Hopf bifurcation* while the one from E_1 is so-called *secondary Hopf bifurcation* [Yu & Huseyin, 1988]. However, it is noted that the conditions for the incipient Hopf bifurcation are $\mu_2 > 0$, $a_2\mu_1 - \mu_2 < 0$, and $a_2\mu_1 + (1-a_2^2)\mu_2 = 0$, which is not possible since $a_2^2 < 2$. Therefore, there is no Hopf bifurcation from E_0 . On the other hand, the secondary Hopf bifurcation from E_1 may be possible because the conditions $a_2\mu_1 - \mu_2 > 0$ and $a_2\mu_1 + (1-a_2^2)\mu_2 = 0$ may be possible for $\mu_2 < 0$. The static and dynamic bifurcations are shown in the bifurcation diagrams in Fig. 3, where SB and HB denote Static Bifurcation and Hopf Bifurcation, respectively.

Next, we discuss the periodic solution (limit cycle) (w_2, r_2) . First consider the existence of this solution, which requires non-negative discriminant of Eq. (27),

$$\begin{aligned} \Delta &= A_1^2 - 4A_2 \\ &= \frac{64a_2^2(2-a_2^2)^2}{(1+4a_2^2)^2} \left[\left(a_2\mu_1 - \mu_2 + \frac{4a_2^3(2-a_2^2)}{1+4a_2^2} \right)^2 \right. \\ &\quad \left. - \frac{16a_2(2-a_2^2)}{1+4a_2^2} (a_2\mu_1 + (1-a_2^2)\mu_2) \right] \\ &\geq 0, \end{aligned}$$

under which the periodic solution is

$$\begin{aligned} r_{2\pm}^2 &= \frac{1}{2} \left[\frac{8(2-a_2^2)^2}{a_2(1+4a_2^2)} \right. \\ &\quad \left. \times \left(a_2\mu_1 + \mu_2 - \frac{4a_2^5}{1+4a_2^2} \right) \pm \sqrt{\Delta} \right], \quad (29) \end{aligned}$$

and $w_{2\pm}$ is then given by (26). Now, in order to have a stable periodic solution bifurcating from E_1 , it requires $\mu_2 < 0$, $a_2\mu_1 - \mu_2 > 0$ and $a_2\mu_1 + (1-a_2^2)\mu_2 < 0$, which yields

$$\begin{aligned} a_2\mu_1 + \mu_2 - \frac{4a_2^5}{1+4a_2^2} &< a_2^2\mu_2 - \frac{4a_2^5}{1+4a_2^2} \\ &< 0 \quad \text{for } \mu_2 < 0. \end{aligned}$$

Therefore, $r_{2-}^2 < 0$, yielding no real solution; while the existence of real positive solution r_{2+}^2 needs $A_2 < 0$, which in turn gives $a_2(1-a_2^2)\mu_1 + \mu_2 > 0$.

Define the critical line,

$$L_3: a_2(1-a_2^2)\mu_1 + \mu_2 = 0 \quad (30)$$

which shows the boundary of the existence of periodic solutions. These three critical lines L_k , $k = 1, 2, 3$ are depicted in the bifurcation diagrams in Fig. 3. It is clearly shown that there cannot exist the secondary Hopf bifurcation since the equilibrium solution E_1 would hit the existence boundary L_3 before crossing the secondary Hopf bifurcation line L_2 . Summarizing the above results we conclude that there are no periodic solutions (limit cycles) around the origin due to zero-Hopf bifurcation. Hence, both Hopf bifurcations, though indicated in the diagrams in Fig. 3, actually do not occur due to parameter restriction. ■

The bifurcation diagrams shown in Fig. 3, obtained based on zero-Hopf bifurcation at E_0 can also be applied for the zero-Hopf bifurcation at equilibrium E_1 as long as the two notations E_0 and E_1 in these diagrams are exchanged.

We have used simulation to verify the above analytical results. For the various values of a_2 chosen from four categories (see Fig. 3), we can always find that the trajectories starting from the initial points in the stable regions of E_0 and E_1 converge to E_0 or E_1 . However, we did not find any simulated stable periodic solutions around the origin in the vicinity of the zero-Hopf critical point. In fact, for the parameter values not chosen from the two stable regions, all trajectories diverge to infinity.

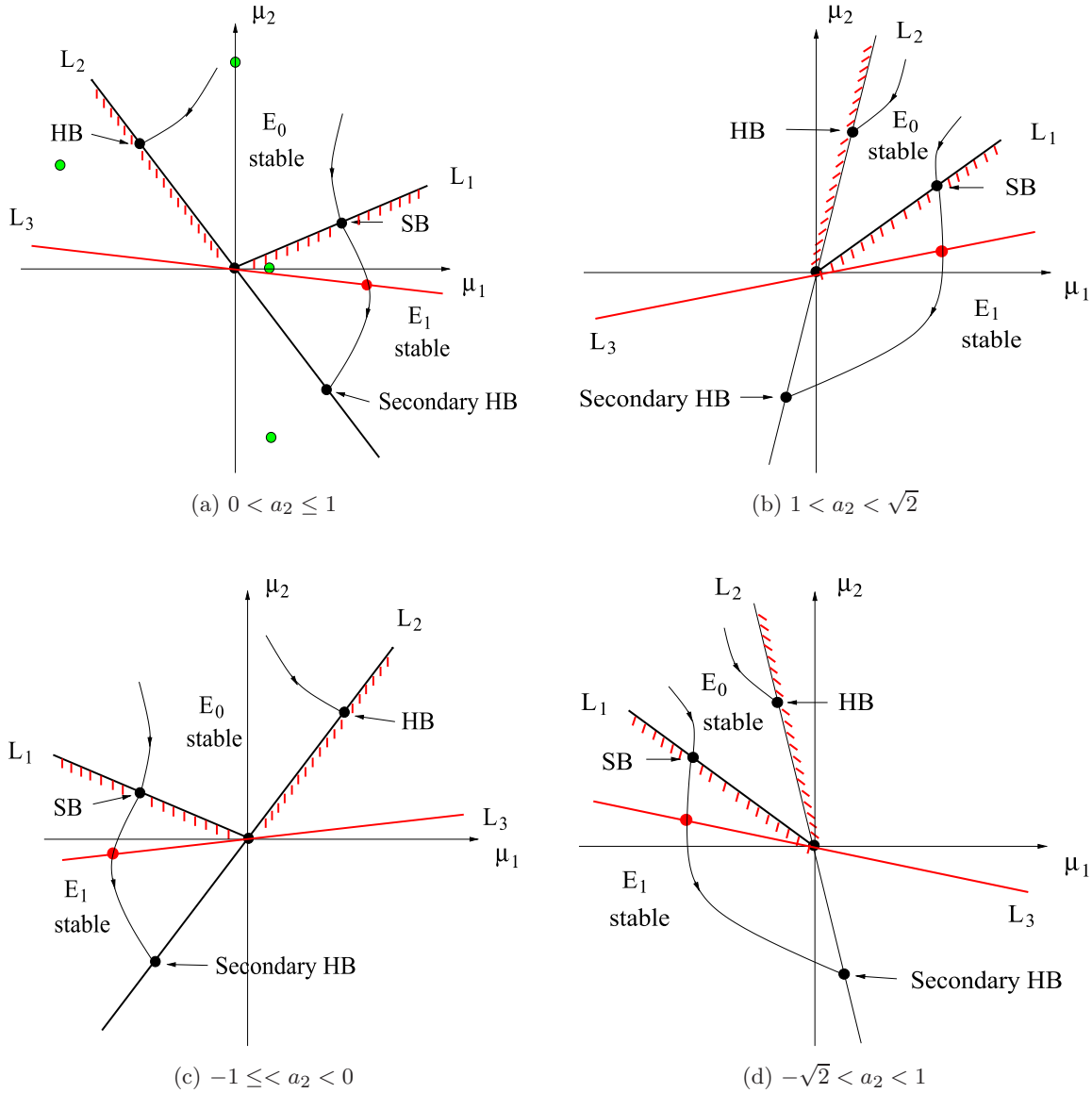


Fig. 3. Zero-Hopf bifurcation diagrams of system (2) at E_0 for Case (A).

To illustrate the above results, we present simulations for $a_2 = \frac{1}{2}$, which belong to the case in Fig. 3(a). For this value of a_2 , the critical lines become

$$\begin{aligned}
 L_1 : \mu_2 &= \frac{1}{2}\mu_1, \\
 L_2 : \mu_2 &= -\frac{2}{3}\mu_1, \\
 L_3 : \mu_2 &= -\frac{3}{8}\mu_1.
 \end{aligned}$$

We choose four sets of parameter values for (μ_1, μ_2) :

$$\begin{aligned}
 (\mu_1, \mu_2) &= (0, 0.01), \quad (0.001, 0), \\
 &(-0.01, 0.005), \quad (0.001, -0.01),
 \end{aligned}$$

which are indicated in Fig. 3(a) as green filled circles. The initial point is taken as $(x, y, z) = (0.001, 0.001, 0)$ for all four simulations. The simulation results are depicted in Figs. 4(a)–4(d), respectively. It is clearly shown in Fig. 4(a) that the trajectory starting from the initial point located in the stable region of E_0 [see Fig. 3(a)] converges to the origin. Figure 4(b) indicates that the trajectory starting from the initial point located in the stable region of E_1 converges to the nonzero equilibrium $(x, y, z) = (-0.0005, 0.001, -0.001)$, which can be easily verified as the equilibrium of system (2). When the two parameter values are chosen on the left side of the critical line L_2 [see Fig. 3(a)], both trajectories diverge to infinity no matter how the

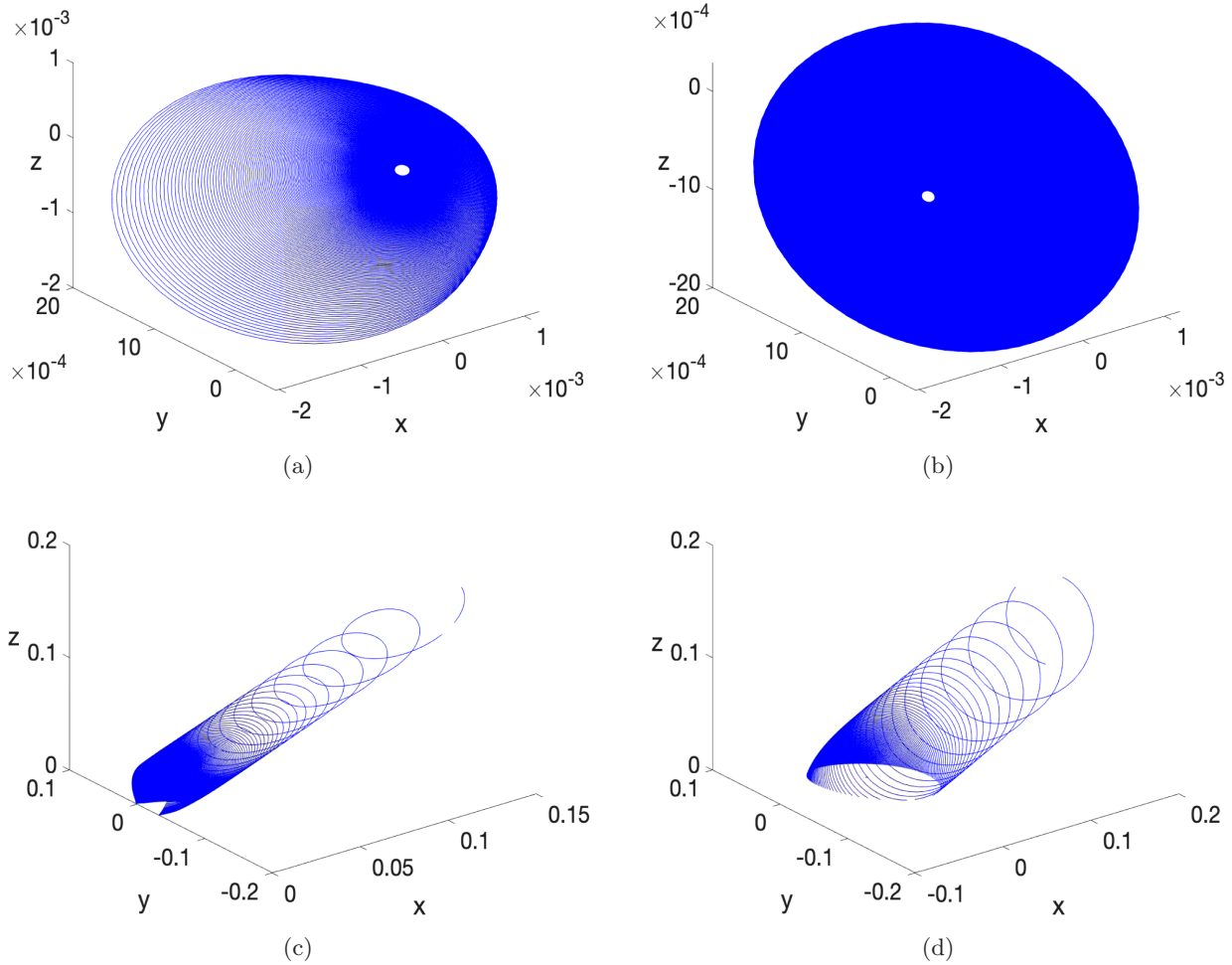


Fig. 4. Simulations of Case (A) of system (2) for the parameter values: $a_2 = 0.5$, $b_2 = 1 + \mu_1$, $c_2 = 0.5 + \mu_2$, with the initial condition $(x_0, y_0, z_0) = (0.001, 0.001, 0)$: (a) $(\mu_1, \mu_2) = (0, 0.01)$, converging to E_0 , (b) $(\mu_1, \mu_2) = (0.001, 0)$, converging to E_1 , (c) $(\mu_1, \mu_2) = (0.001, -0.01)$, diverging to infinity and (d) $(\mu_1, \mu_2) = (-0.01, 0.005)$, diverging to infinity.

initial points are chosen close to the origin, as seen in Figs. 4(c) and 4(d).

Moreover, it is noted that unlike the Rössler system (1) for which all trajectories globally converge to the stable limit cycle, the equilibrium solutions E_0 and E_1 of system (2) are only locally asymptotically stable, and very sensitive to the initial conditions. For example, for the first set of parameter values $(\mu_1, \mu_2) = (0, 0.01)$, if we change the initial point from $(0.001, 0.001, 0)$ to $(0.1, 0.1, 0)$, then the trajectory no longer converges to the origin but diverges to infinity. Similarly, for the second set of parameter values $(\mu_1, \mu_2) = (0.001, 0)$, if we change the initial point from $(0.001, 0.001, 0)$ to $(0.01, 0.01, 0)$, then the trajectory does not converge to the nonzero equilibrium but diverges to infinity.

We notice that in Theorem 2.1 of [Llibre, 2014] (and the proof, based on the time-averaging method, is given in Sec. 4, see Proof 6) conditions

are given for the existence of periodic solutions from the zero-Hopf bifurcation. Since no simulations are provided in [Llibre, 2014], we cannot verify Theorem 2.1 in [Llibre, 2014]. The discrepancy between Theorem 2.1 in [Llibre, 2014] and our result may be caused by the stability conditions.

3.2. Zero-Hopf bifurcation at E_0 for Case (B)

We now turn to Case (B), for which we have the following result.

Theorem 4. *From the equilibrium E_0 of system (2), zero-Hopf bifurcation occurs at the critical point $a_2 = c_2 = 0$, ($b_2 > -1$). The static bifurcation occurs in the vicinity of this critical point, yielding a nonzero equilibrium solution E_1 . Hopf bifurcation is not possible and no periodic solutions exist around this zero-Hopf critical point.*

Proof. We take perturbations from the zero-Hopf critical point as

$$\begin{aligned} a_2 &= 0 + \mu_1 = \mu_1, \\ c_2 &= 0 + \mu_2 = \mu_2, \\ b_2 &> -1, \quad 0 < |\mu_1|, |\mu_2| \ll 1. \end{aligned} \tag{31}$$

Then, we apply the following linear transformation ($b_2 \neq 0$, when $b_2 = 0$, the system becomes degenerate with a singular line $z = -y$ on the $y-z$ plane),

$$\begin{pmatrix} x \\ y \\ z \end{pmatrix} = \begin{bmatrix} 0 & \frac{\sqrt{1+b_2}}{b_2} & 0 \\ \frac{1}{b_2} & 0 & 1 \\ 1 & 0 & -1 \end{bmatrix} \begin{pmatrix} u \\ v \\ w \end{pmatrix}$$

to system (2) to obtain

$$\begin{aligned} \dot{w} &= \frac{1}{1+b_2}(b_2\mu_1 - \mu_2)w + \frac{1}{b_2\sqrt{1+b_2}}(w-u)v, \\ \dot{u} &= \sqrt{1+b_2}v + \frac{1}{1+b_2}(\mu_1 - b_2\mu_2)u \\ &\quad - \frac{1}{\sqrt{1+b_2}}(w-u)v, \\ \dot{v} &= -\sqrt{1+b_2}u. \end{aligned} \tag{32}$$

Now applying the Maple program of computing the normal form associated with zero-Hopf bifurcation [Bi & Yu, 1999; Tian & Yu, 2014] to the above system (setting $\mu_1 = \mu_2 = 0$), we obtain

$$\begin{aligned} \dot{w} &= \frac{1}{1+b_2}(b_2\mu_1 - \mu_2)w, \\ \dot{r} &= \frac{1}{2(1+b_2)}(\mu_1 - b_2\mu_2)r, \\ \dot{\theta} &= \sqrt{1+b_2} - \frac{1}{2\sqrt{1+b_2}}w - \frac{1}{8(1+b_2)^{3/2}}w^2 \\ &\quad - \frac{3+2b_2}{48b_2(1+b_2)^{3/2}}r^2, \end{aligned} \tag{33}$$

which shows that $\dot{w} = \dot{r} = 0$ without the unfolding terms. Hence, there does not exist periodic solutions near this zero-Hopf critical point. As a matter of fact, it can be shown that at $\mu_1 = \mu_2 = 0$,

system (32) has an algebraic integral curve, given by

$$f(w, u, v) = u - w + b_2, \tag{34}$$

which is called Darboux polynomial of system (32) with $\mu_1 = \mu_2 = 0$. Let

$$\begin{aligned} P &= \frac{1}{b_2\sqrt{1+b_2}}(w-u)v, \\ Q &= \sqrt{1+b_2}v - \frac{1}{\sqrt{1+b_2}}(w-u)v, \\ R &= -\sqrt{1+b_2}u, \end{aligned}$$

which represents the vector field of system (32) without unfolding. Then it is easy to show that

$$\begin{aligned} \frac{\partial f}{\partial w}P + \frac{\partial f}{\partial u}Q + \frac{\partial f}{\partial v}R \\ = (u-w+b_2)\frac{\sqrt{1+b_2}}{b_2}v \\ = f(w, u, v)K(w, u, v), \end{aligned}$$

where $K = \frac{\sqrt{1+b_2}}{b_2}v$ is called the cofactor of the system associated with the polynomial f . ■

Finally, we use simulations by taking different parameter values to verify the above results. First note that for a set of parameter values, there always exist two equilibria E_0 and E_1 . The two unfolding terms in the first two equations of the normal form (33) are associated with the zero-Hopf bifurcation around $E_0 = (0, 0, 0)$. A necessary condition for the equilibrium to be stable is $\mu_2 - b_2\mu_2 < 0$ under which E_0 is asymptotically stable if $b_2\mu_1 - \mu_2 < 0$. When $b_2\mu_1 - \mu_2 > 0$, E_0 becomes unstable and bifurcates into the stable equilibrium E_1 . The detailed parameter values are given in Table 1, in which the convergence/divergence of simulated trajectories are also listed. In particular, convergence to the equilibria E_0 and E_1 are indicated by the red and green colors, respectively, distinguishing them from all other cases with trajectories diverging to infinity. It is seen that the necessary condition $\mu_2 - b_2\mu_2 < 0$ must hold for the convergence to E_0 and E_1 , and the sign of $b_2\mu_1 - \mu_2$ then determines to which equilibrium the trajectory converges.

Simulations with the parameter values in Table 1 are given in Fig. 5, which indeed show an excellent agreement with the analytical predictions listed in Table 1. However, it should be noted that the asymptotic convergence to the equilibria

Table 1. Parameter values for simulating Case (B) of system (2).

b_2	$a_2 = \mu_1$	$c_2 = \mu_2$	$b_2\mu_1 - \mu_2$	$\mu_1 - b_2\mu_2$	Initial Point	Convergence/Divergence
-0.5	-0.02	0.03	< 0	< 0	(0.1, 0.1, -0.1)	E_0
-0.5	-0.02	0.005	> 0	< 0	(0.1, 0.1, -0.04)	E_1
-0.5	-0.02	0.05	< 0	> 0	(0.0001, 0, 0)	∞
-0.5	0.02	-0.03	> 0	> 0	(0.0001, 0, 0)	∞
0.5	0.02	0.05	< 0	< 0	(0.1, 0.1, -0.1)	E_0
0.5	-0.02	-0.03	> 0	< 0	(0.0001, 0, 0)	E_1
0.5	0.02	0.03	< 0	> 0	(0.0001, 0, 0)	∞
0.5	0.02	0.005	> 0	> 0	(0.0001, 0, 0)	∞

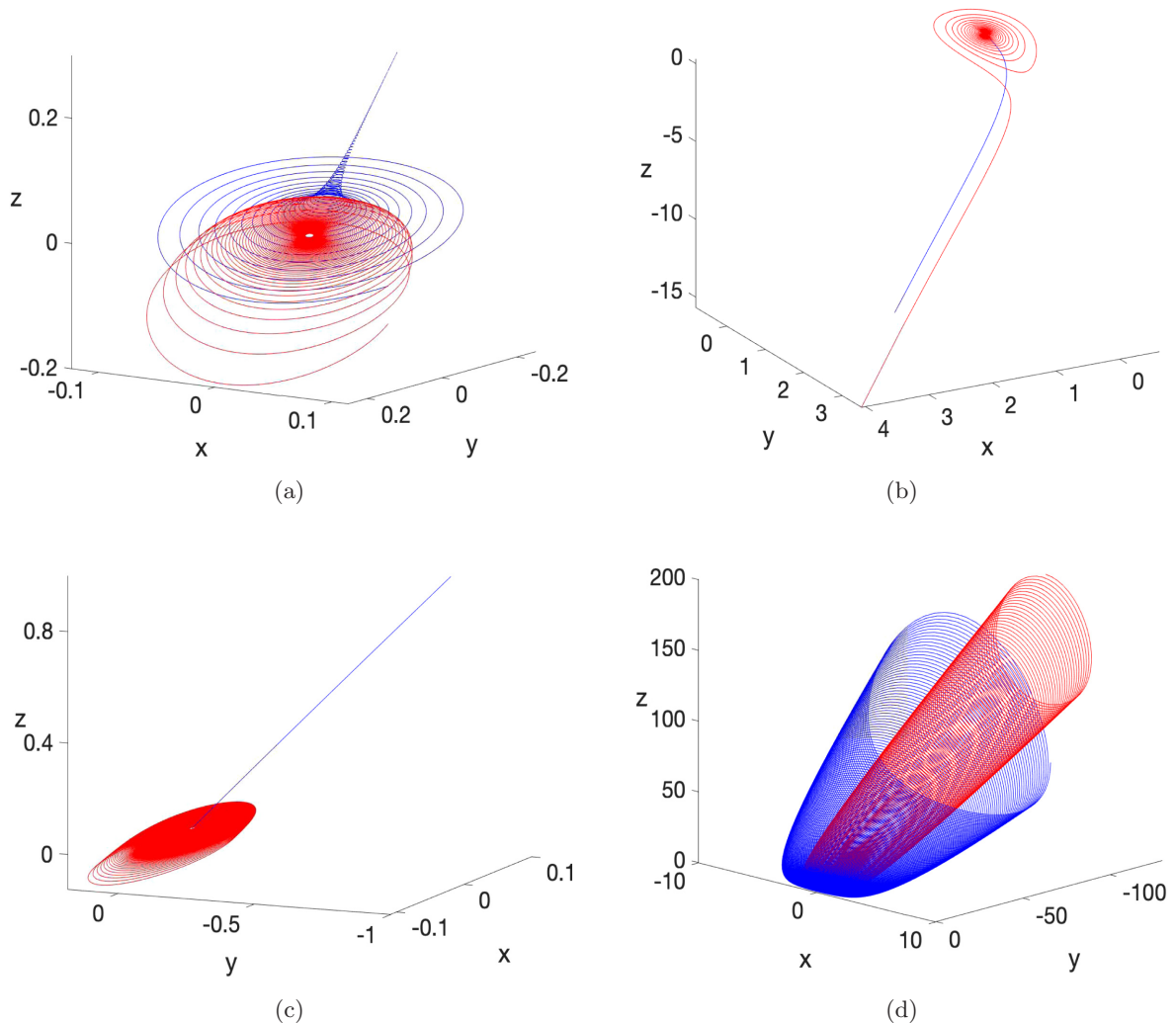


Fig. 5. Simulations of Case (B) of system (2) for (a) $(a_2, b_2, c_2) = (-0.02, -0.5, 0.03)$, converging to E_0 (red orbit) from $(x_0, y_0, z_0) = (0.1, 0.1, -0.1)$, and $(a_2, b_2, c_2) = (-0.02, -0.5, 0.005)$, converging to E_1 (blue orbit) from $(x_0, y_0, z_0) = (0.1, 0.1, -0.04)$; (b) $(a_2, b_2, c_2) = (-0.02, -0.5, 0.05)$ and $(a_2, b_2, c_2) = (-0.02, -0.5, -0.03)$, diverging to infinity from $(x_0, y_0, z_0) = (0.0001, 0, 0)$ (red and blue orbits); (c) $(a_2, b_2, c_2) = (0.02, 0.5, 0.05)$, converging to E_0 (red orbit) from $(x_0, y_0, z_0) = (0.1, 0.1, -0.1)$, and $(a_2, b_2, c_2) = (-0.02, 0.5, -0.03)$, converging to E_1 (blue orbit) from $(x_0, y_0, z_0) = (0.0001, 0, 0)$ and (d) $(a_2, b_2, c_2) = (0.02, 0.5, 0.03)$ and $(a, b, c) = (0.02, 0.5, 0.005)$, diverging to infinity from $(x_0, y_0, z_0) = (0.0001, 0, 0)$ (red and blue orbits).

E_0 and E_1 is local. For example, for the parameter values $(a_2, b_2, c_2) = (-0.02, -0.5, 0.03)$ (see the first row in Table 1), when the initial point is changed from $(x_0, y_0, z_0) = (0.1, 0.1, -0.1)$ to $(1, 1, -1)$, the trajectory diverges to infinity, rather than converging to E_0 . For the parameter values $(a_2, b_2, c_2) = (-0.02, 0.5, -0.03)$ (see the sixth row in Table 1), when the initial point is changed from $(0.0001, 0, 0)$ to $(0.1, 0.1, -0.1)$, the trajectory diverges to infinity, rather than converging to E_1 .

4. Conclusion

In this paper, we have applied normal form theory to reinvestigate zero-Hopf bifurcations in two Rössler systems which are not equivalent. It is shown that the periodic orbits bifurcating from the zero-Hopf critical point are actually from Hopf bifurcation and the bifurcating limit cycles can be stable or unstable, depending upon parameter values. The results obtained in this paper indicate that unstable limit cycles cannot be detected by the time-averaging method, but can be determined by using the normal form method.

Acknowledgment

This work was supported by the Natural Sciences and Engineering Research Council of Canada (No. R2686A02).

References

Bi, Q. & Yu, P. [1999] "Symbolic computation of normal forms for semi-simple cases," *J. Comput. Appl. Math.* **102**, 195–220.

- Guckenheimer, J. & Holmes, P. [1993] *Nonlinear Oscillations, Dynamical Systems, and Bifurcations of Vector Fields*, 4th edition (Springer, NY).
- Han, M. & Yu, P. [2012] *Normal Forms, Melnikov Functions, and Bifurcations of Limit Cycles* (Springer, NY).
- Kuznetsov, Y. [2004] *Elements of Applied Bifurcation Theory* (Springer, NY).
- Llibre, J. [2014] "Periodic orbits in the zero-Hopf bifurcation of the Rössler system," *Romanian Astron. J.* **24**, 49–60.
- Llibre, J. & Makhlouf, A. [2020] "Zero-Hopf periodic orbits for a Rössler differential system," *Int J. Bifurcation and Chaos* **30**, 2050170-1–6.
- Rössler, O. E. [1976] "An equation for continuous chaos," *Phys. Lett. A* **57**, 397–398.
- Tian, T. & Yu, P. [2014] "An explicit recursive formula for computing the normal forms associated with semisimple cases," *Commun. Nonlin. Sci. Numer. Simulat.* **19**, 2294–2308.
- Yu, P. [1998] "Computation of normal forms via a perturbation technique," *J. Sound Vibr.* **211**, 19–38.
- Yu, P. & Huseyin, K. [1988] "A Perturbation analysis of interactive static and dynamic bifurcations," *IEEE Trans. Autom. Contr.* **33**, 28–41.
- Yu, P. & Yuan, Y. [2001] "The simplest normal form for the singularity of a pure imaginary pair and a zero eigenvalue," *Dyn. Cont. Discr. Impuls. Syst. Ser. B* **8**, 219–249.
- Yu, P. & Chen, G. [2004] "Hopf bifurcation control using nonlinear feedback with polynomial functions," *Int. J. Bifurcation and Chaos* **14**, 1683–1704.